Supplementary Information

A Novel CEST-Contrast Nanoagent for Differentiating the Malignant Degree in Breast Cancer

Authors: Bixue Chen[a], Xianfu Meng[b,c], Wanlu Wu[a], Yuwen Zhang[d], Lin Ma[a], Kaidong Chen[a] and Xiangming Fang*[a]

[a]*Department of Radiology, The Affiliated Wuxi People's Hospital of Nanjing Medical University, Wuxi, China.*

[b]*Department of Medical Ultrasound, Shanghai Tenth People's Hospital, School of Medicine, Tongji University, Shanghai, China.*

[c]*Department of Materials Science and State Key Laboratory of Molecular Engineering of Polymers, Fudan University, Shanghai, China.*

[d]*Institute of Science and Technology for Brain-Inspired Intelligence, Fudan University, Shanghai, China*

* Correspondence: Xiangming Fang, xiangming_fang@njmu.edu.cn
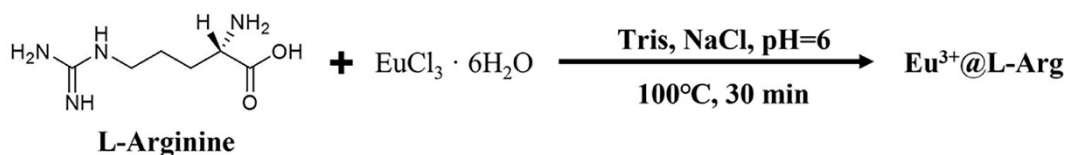
Supplementary Figures:

Figure S1. Flow chart of Eu^{3+}@L-Arg preparation.

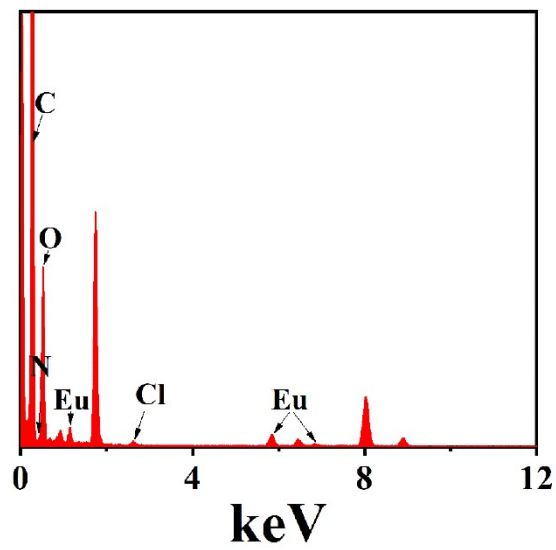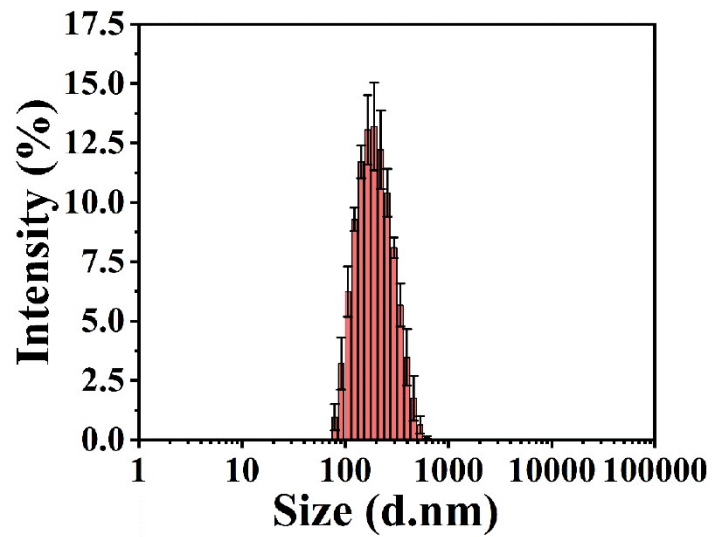Figure S2. EDS elemental analysis of Eu^{3+}@L-Arg.

Figure S3. Dynamic light scattering (DLS) of Eu^{3+}@L-Arg (Z-average: 176.9 nm, PDI: 0.09, pH= 7.4). All experiments were performed at least three times.
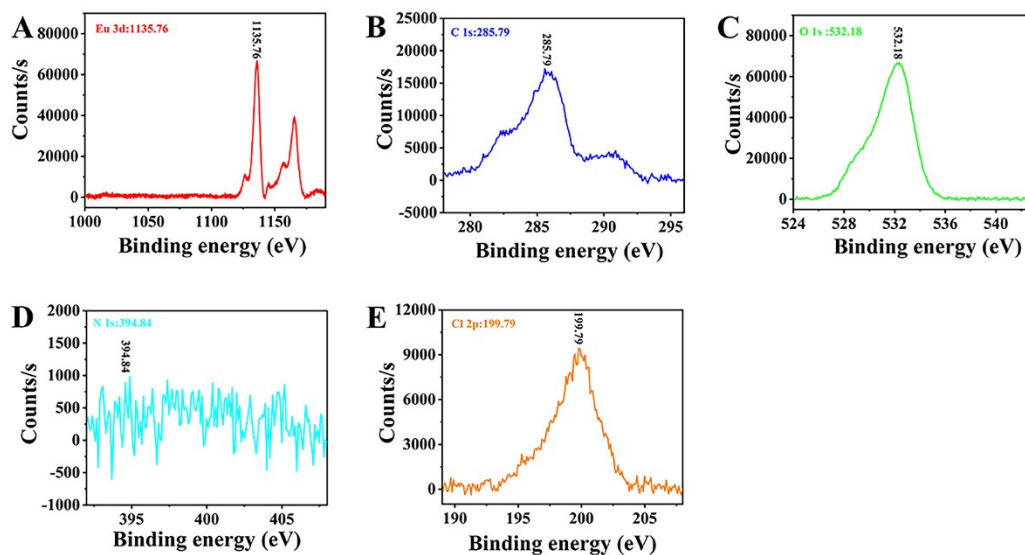
Figure S4. (A) XPS spectra of Eu 3d: 1135.76; (B) C 1s: 285.79; (C) O 1s: 532.18; (D) N 1s: 395.40; (E) Cl 2p: 199.79.

Experimental projects		pH	Average (nm)	SD
TEM		7.4	120.5	1.04
DLS	Size	5.6	178.9	3.52
		6.0	174.8	2.17
		6.4	173.3	2.32
		6.8	173.6	1.01
		7.0	175.8	1.82
		7.4	176.9	1.40
	Zeta Potential	5.6	43.1	0.49

		6.0	43.1	0.46
		6.4	42.5	1.68
		6.8	41.7	4.48
		7.0	43.1	1.59
		7.4	42.3	5.52

Figure S5: TEM (pH = 7.4, n = 3) and DLS data of Eu^{3+}@L-Arg nanomaterials in different pH buffer (pH = 5.6, 6.0, 6.4, 6.8, 7.0, 7.4, n = 3). All experiments were performed at least three times.
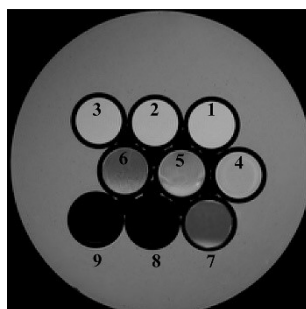

Figure S6. T2 magnetic resonance imaging of Eu^{3+}@L-Arg nanomaterials with different concentrations (1-9: 0, 8, 16, 32, 62.5, 125, 250, 500, 1000 μg/mL). All experiments were performed at least three times.
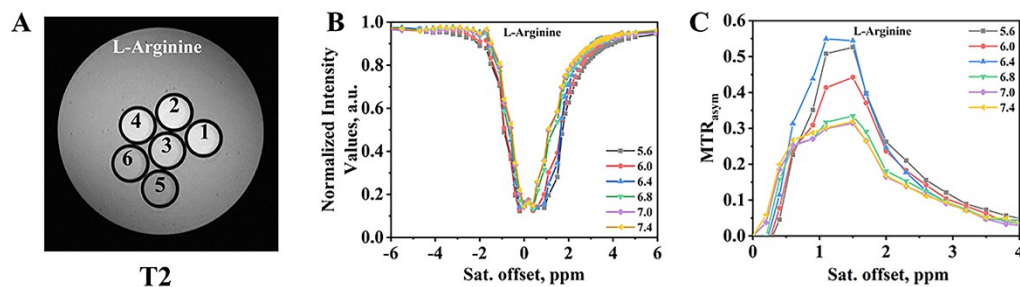

Figure S7. (A) T2 image of L-Arginine (62.5 μg/mL) in Hepes buffers of different pH (1-6: 5.6, 6.0, 6.4, 6.8, 7.0, 7.4); (B) Z spectra of L-Arginine in Hepes buffers of different pH; (C) MTR$_{asym}$ spectra

of L- Arginine in Hepes buffers of different pH. All subpanels reflect representative data from experiments repeated three times ($B_0 = 11.7$ T, $B_1 = 10$ μT). All experiments were performed at least three times.
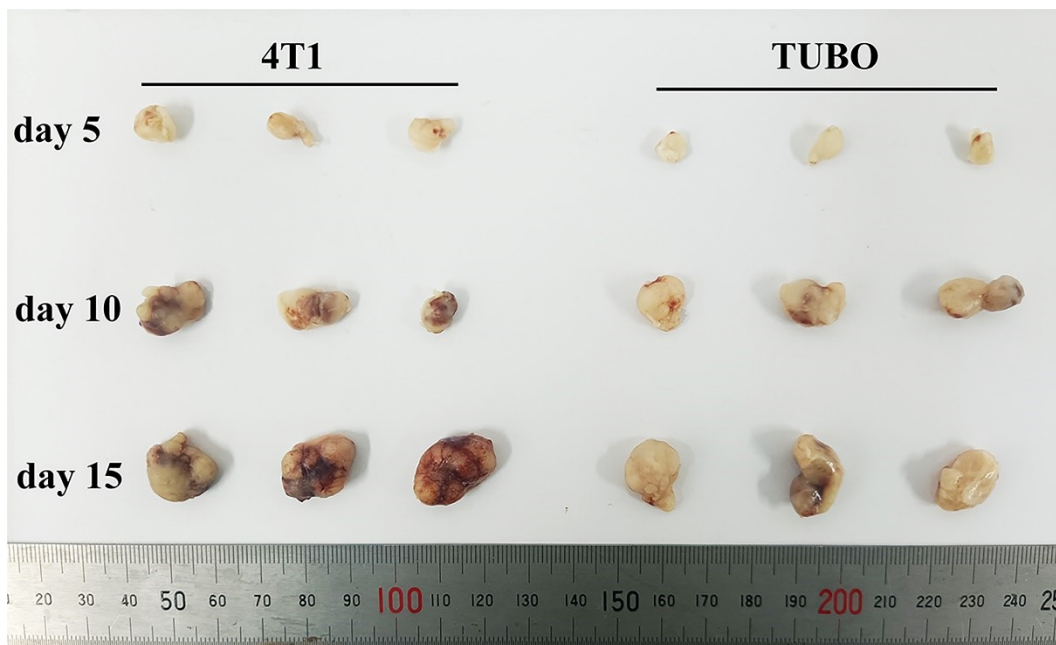

Figure S8. Tumor volumes of 4T1 and TUBO cells at day 5, day10 and day 15 after injection subcutaneously into nude mice (n = 3).
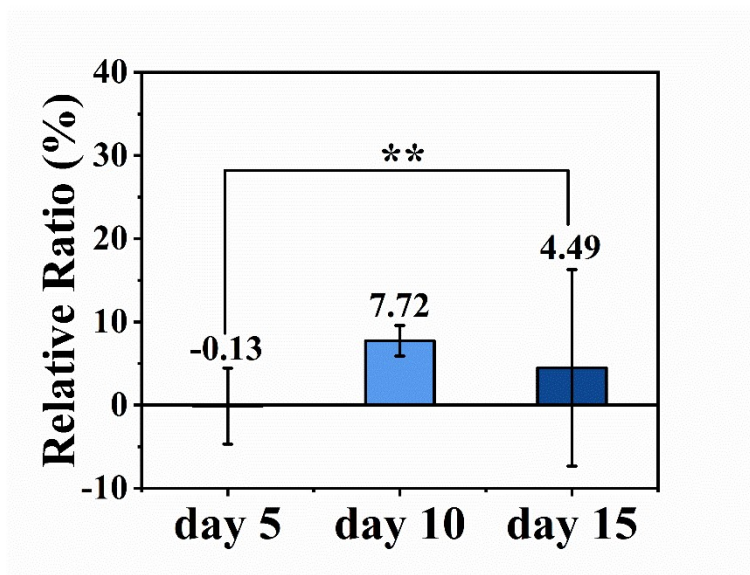
Figure S9. Relative signal change rate of CEST MTRaysm before and after Eu^{3+}@L-Arg nanomaterials injection at 17.0 ppm for three groups of TUBO breast cancers (day 5, day 10 and day 15, B_0 = 11.7 T, B_1 = 10 µT, n = 3, mean ± SD).
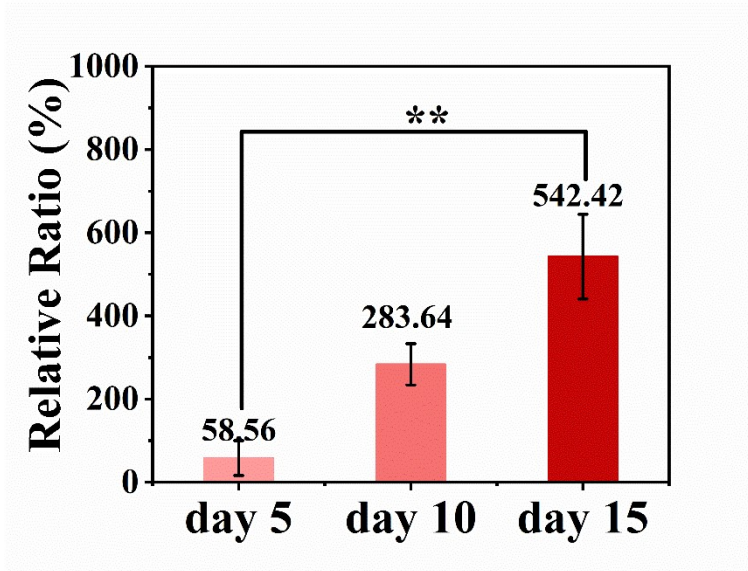

Figure S10. Relative signal change rate of CEST MTR$_{aysm}$ before and after Eu^{3+}@L-Arg nanomaterials injection at 17.0 ppm for three groups of 4T1 breast cancers (day 5, day 10 and day 15, B_0 = 11.7 T, B_1 = 10 µT, n = 3, mean ± SD).
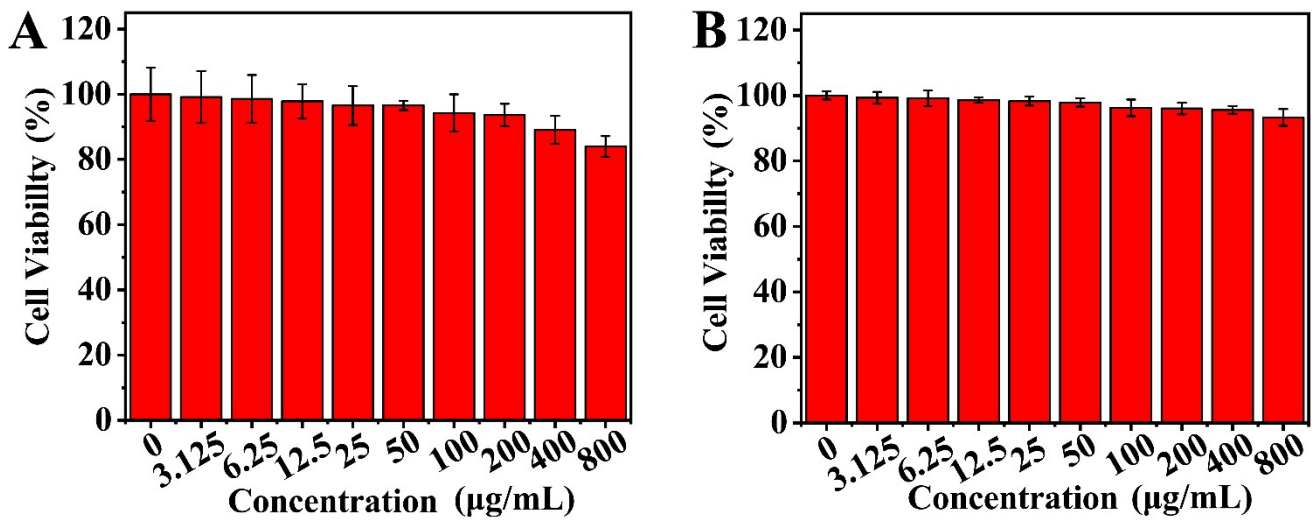
Figure S11. Cell viability of TUBO (A) and 4T1 (B) cells cultured with different concentrations of Eu^{3+}@L-Arg nanomaterials at 0, 3.125, 6.25, 12.5, 25, 50, 100, 200, 400, 800 µg/mL (n = 6, mean ± SD). All experiments were performed at least three times.

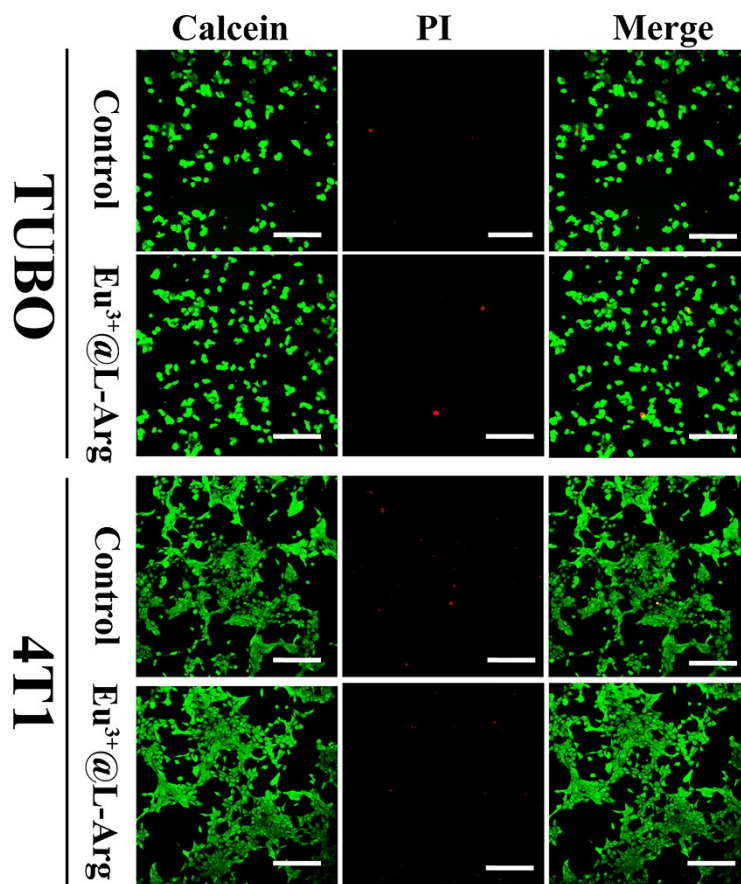

Figure S12. Confocal fluorescence images of TUBO and 4T1 cells co-stained with calcein-AM and PI after incubated with Eu^{3+}@L-Arg nanoparticles (Eu: 800 µg/mL, 24 h). The scale bar was 100 µm. All subpanels reflect representative data from experiments repeated three times.
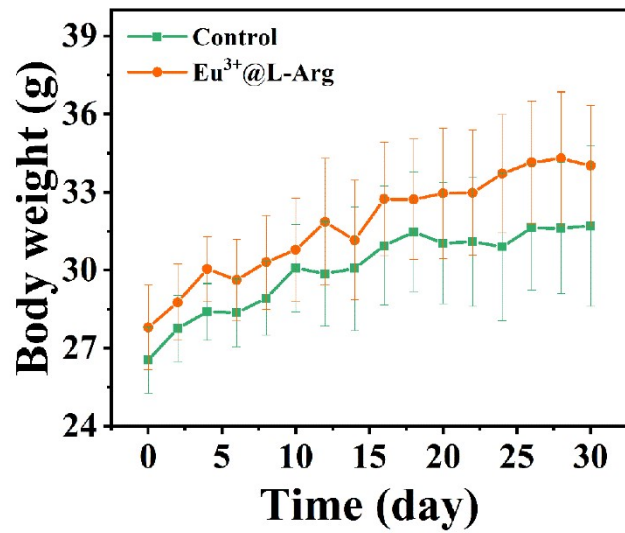
Figure S13. Body weight variation after 30 days of Eu³⁺@L-Arg nanomaterials injection, with 0.9% NaCl injection as control (n = 5, mean ± SD).
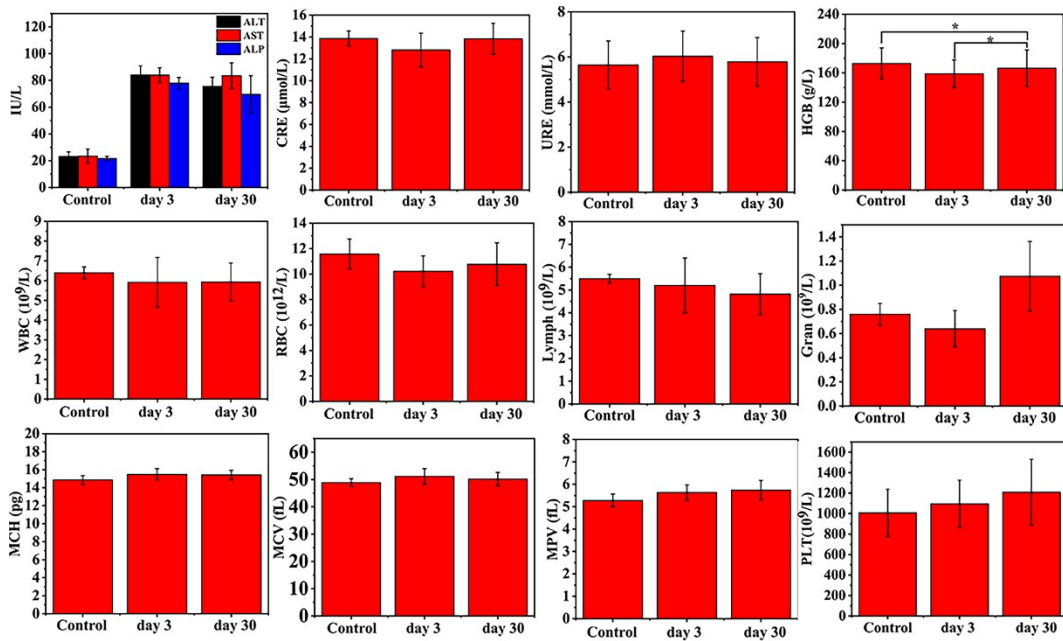

Figure S14. Blood biochemical and hematological analysis of ICR mice after 3 and 30 days of Eu³⁺@L-Arg nanomaterials injection (20mg/ kg, 100 μL), with 100 μL of 0.9% NaCl injection as control (n = 5, $P < 0.05$).
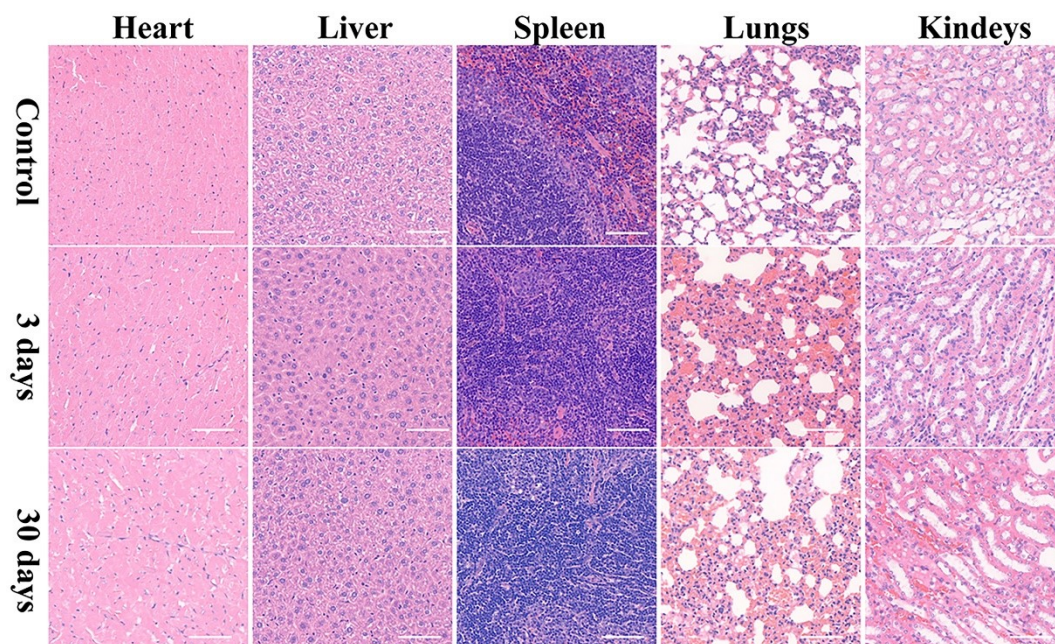
Figure S15. H&E staining analysis of the heart, liver, spleen, lungs and kidneys after 3 and 30 days of Eu^{3+}@L-Arg nanomaterials injection, with 0.9% NaCl injection as control. The scale bar was 50 μm (n = 5).